The International Archives of the Photogrammetry, Remote Sensing and Spatial Information Sciences, Volume XLVIII-2/W7-2024
Optical 3D Metrology (O3DM), 12–13 December 2024, Brescia, Italy

Optimizing Incidence Angle and Range for Single-Shot Laser Scanning Point Clouds to Model Aerospace Fasteners

Kate Pexman, Stuart Robson

Dept. of Geomatic Engineering, University College London, Gower Street, London, WC1E 6BT, United Kingdom – uceskkp@ucl.ac.uk

Technical Commission II

Keywords: Laser Scanning, 3D Reconstruction, Aerospace Manufacturing, Feature Detection

Abstract

In high-precision manufacturing environments, optical metrology technologies allow on-line checking and validation, offering live digital representations, with the broader potential to create digital manufacturing twins. An established typical aerospace application involves the alignment of assemblies where components need to be compared against design tolerances at key manufacturing stages. Accurate, precise and reliable measurement tools such as laser trackers are the popular choice for such processes in large-volume manufacturing settings. A critical aerospace challenge follows alignment, drilling and fastening operations enabling surface covers to be attached to underpinning structures, where the smallest manufacturing variations can cause excess drag impacting aerodynamic performance. Determining surface conformance of airstream facing surfaces challenges laser tracker systems which, whilst capable of localised surface scanning, require costly large volume robotics to productively measure large wing surfaces at high levels of local detail. This technology gap creates opportunity for the use of 3D imaging devices such as medium range laser scanners and detection strategies such as automated feature detection from point clouds. In this work, various laser scanner devices were used to detect fasteners of different sizes on a fastener sample plate from a single shot setup. This fastener sample plate is representative of a typical aerospace surface and is comprised of common aerospace materials. Highly precise measurements, in the range of 0.5 mm were achieved, and conclusions were drawn about optimal range and incidence angle for both aerodynamic and interior sides of an aerospace surface.

1. Introduction

While the use of laser trackers in an aerospace manufacturing context is relatively commonplace, industry has been much slower to adopt laser scanners and point cloud data with the same readiness. This is mainly because the vast majority of laser scanners are not designed for high-precision measuring tasks, rather they focus on amount of achievable coverage with a standard accuracy tolerance. Exploring the limits of medium range laser scanners when used in non-optimal situations can allow for the discovery of the true capabilities of these devices in real manufacturing scenarios.

Automated feature detection is an established concept in the field of 3D imaging and analysis. Instruments such as laser scanners have been used for decades to capture point cloud datasets of physical environments. These point clouds are then analysed using various domain specific methods in order to extract useful information. Successful extraction methods can be broken down into learning-based and logic-based decision structures. In learning-based models, prior data is used to train a detection learning system to recognise features within a point cloud. This requires a library of preclassified features or a populated database with semantic labelling, often neither being practical in real scenarios. Alternatively, in logic-based models, sometimes referred to as hard-coded models (Wang, Tan, and Mei 2020), the decisions themselves are based on structures and patterns in the data. These structures and patterns represent recognisable shapes such as planes, lines and circles, often referred to as geometric primitives (Roth and Levine 1993). Their contextual and spatial relationships are used to inform complex decision structures that can make inferences to produce semantic labelling.

In an aerospace manufacturing context, sub-millimetre thresholds for data accuracy are often required. Whereas laser trackers and photogrammetric systems can often achieve the requisite precision, they do not provide the same large volume full-field surface coverage that can be produced with a laser scanner. An additional constraint is the geometry of the assembly setup and the speed at which the data needs to be captured. These factors influenced the decision to test single-shot scanning in this work, i.e. only one scan is captured and therefore no point cloud registration is required. The successes and difficulties of single shot scanning will be discussed and analysed in subsequent sections.

In previous works involving feature detection, described in the literature review, the focus has been on quantity of features detected rather than on quality. Few studies using point cloud data have achieved sub-millimetre detection of features using mid-range terrestrial laser scanners. Additionally, aerospace materials are often non-ideal for laser-based measurements, due to their variations in reflectivity and underlying curved surface forms. Highly variant incidence angles experienced in the manufacturing environment further contribute to challenges in automated feature detection. A robust feature detection system should be designed to accommodate changes in the intensity, colour, range or incidence angle to the measured object.

In this work, two standard consumer grade terrestrial laser scanners are used to capture an aerospace fastener sample plate. This object has a flush aerodynamic side to comply with airflow requirements, and an interior side that holds protruding fasteners. These two sides of the sample plate provide their own unique challenges which must be overcome to produce a single-scan solution able to detect features on the workpiece. To evaluate scanner and extraction capabilities, experiments have been designed which alter the incidence angle and the range of a series of single-scan setups. The quality of the detected features is analysed by comparing estimated values with a reference set of values extracted from measurements taken with a high-precision laser-tracker tracked hand-held scanner. The detection rate is presented, and the repeatability of the solution is examined through standard deviations of the repeated features. Finally, preliminary work has been carried out to estimate the alignment of each fastener on the aerodynamic side of the fastener sample plate.

The following section contains a literature review on both geometric primitive detection and feature identification in an aerospace context. Detailed methodology is presented in Section 3, followed by the results of various experiments with the two tested scanners in Section 4. Conclusions are drawn in Section 5 and areas of future work are identified.

2. Literature Review

Extracting geometric primitives began with range data, captured by early versions of machines which would subsequently form the blueprint for modern laser scanners. One of the essential developments in the field of geometric primitive recognition include Random Sample Consensus (RANSAC) for recognising cylinders in range data (Bolles and Fischler 1981; Fischler and Bolles 1981). Another was the identification of cylinders based on the orientation of their axes from range data (Lozano-Perez, Grimson, and White 1987). Both methods used range data from a light stripe range finder. Crucial least squares approaches to geometric feature detection were developed by (Taubin 1991; Lukács, Martin, and Marshall 1998) where planes, circles, cylinders, lines and ellipses were segmented from 3D range-based data. Development continued as purely range-based scanners began to evolve into more complex machines.

Portions of current literature focus on complete surface reconstruction as opposed to individual feature extraction and measurement. For most applications, complete surfaces are more useful than individual feature points, however feature points can be used in a manufacturing environment for on-line quality control and validation. From an aerospace context, important contributions on individual feature extraction includes the work of (Mineo, Pierce, and Summan 2018) who created a boundary point detection algorithm to replace tessellated surfaces and (Yang et al. 2020) who focused on reverse engineering using subtle features extracted from irregular surfaces.

Many algorithms are designed to detect and fill data voids in point clouds, these data voids are often termed holes. Examples of such algorithms can be found in (Bendels, Schnabel, and Klein 2006) and (Nguyen, Trinh, and Tran 2015). These algorithms often use tessellation to reconstruct holes in the point cloud and replicate the surrounding surface. Implementing geometric primitive detection as a method of identifying and modelling physical holes in a surface from point clouds allows for the location of individual features on a surface that can then be compared with a reference value or known tolerance. Aerospace-specific examples of drill or fastener hole detection include an image-based solution proposed in (Rubio et al. 2017) and a 2D line scanner used to detect tiny holes within an aircraft nacelle (Tang et al. 2022).

Reflective surfaces, such as those found in aerospace manufacturing assembly, can be challenging for laser-based measurement. High-intensity returns can cause gaps and data voids in point clouds, and no algorithm can detect features which are wholly absent from the captured point cloud. There has been a significant amount of work on point cloud correction models for intensity and incidence angle (Pfeifer et al. 2007; Kukko, Kaasalainen, and Litkey 2008; Kaasalainen et al. 2011). Various filtering setups or mathematical systems can be used to correct for the different geometrical attenuations experienced by changing reflectivity of a surface with incidence angle, such as in (Bolkas 2019). However, the intensity correction method for terrestrial scanners is highly dependent on instrumental factors and therefore varies greatly across scanners and systems.

Many manufacturing environments, particularly those in aerospace, comprise complex fixture and assembly spaces where repetitive tasks occur in parallel. Aircraft wings are typically worked on vertically, with the component pieces attached to a supporting fixture. In this orientation, both the aerodynamic and interior aircraft wing structures and surfaces are accessible; with tasks such as assembly, underpinning and affixing happening at the same time. Further information about the assembly of aerospace structures can be found in (Bullen 2013). Scanning such an environment from a single setup is challenging, as ranges and incidence angles can vary in both the horizontal and vertical directions.

3. Method

This paper builds on previously reported work extracting information from drilling templates using laser scanners (Pexman and Robson 2022), where methods from both (Mineo, Pierce, and Summan 2018) and (Tang et al. 2022) were modified and combined to create a feature extraction strategy entitled: M-estimator Sample Consensus – Boundary Point Detection (MSAC-BPD). This algorithm was tested on empty drilling templates, i.e. those not including fasteners. In this second stage paper, fasteners have been added to the drilling templates to replicate a complete aerodynamic surface, and the surface has been scanned from a single setup from both the aerodynamic side and the interior side. Due to these changes to the object of interest, the MSAC-BPD algorithm has been modified to include colour- and intensity-based segmentation. These additional decision structures improve the robustness of the feature extraction algorithm to be able to deal with both drilling templates and surfaces with fasteners.

In this paper, we report on work using a fastener sample plate equipped with various changes in depth and tilt of a series of fasteners. The sample plate is a 10 x 9 grid of fasteners [Figure 1 and Figure 2], varying in size, depth, and tilt. There are three sizes of fasteners, which will be referred to as small, medium and large, and which range from 20-32 mm in diameter. There are thirty fasteners of each size. From a visual inspection, these millimetre and sub-millimetre level changes are difficult to recognize and quantify. The goal of this work is to design a system to recognize changes in these surface characteristics and model the fasteners accurately, using data captured with three different laser scanning instruments [Scanner A, Scanner B and Scanner C]. In order to replicate a manufacturing scenario, both incidence angle and range will be varied for both tested scanners.

This contribution has been peer-reviewed.
https://doi.org/10.5194/isprs-archives-XLVIII-2-W7-2024-113-2024

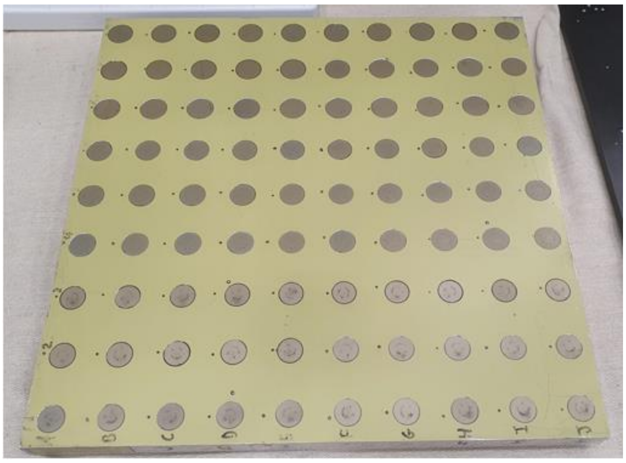

Figure 1: Aerodynamic side of fastener sample plate

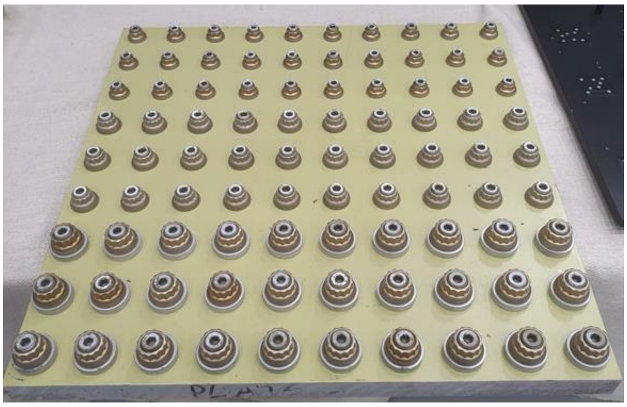

Figure 2: Interior side of fastener sample plate

As seen in Figure 1 and Figure 2, the aerodynamic and interior sides of the fastener sample plate prose different problems from a feature extraction perspective. Fasteners in the sample plate are close together, adding complexity to the problem of decoding individual features when the incidence angle is large.

3.1 MSAC-BPD

The algorithm uses MSAC-BPD, the initial structure set up in (Pexman and Robson 2022). This method first uses MSAC to find a planar section of points from the surface of the fastener sample plate and then looks for holes within that plane. A combination of colour and intensity were added into the extraction algorithm as further decision structures, however not all tested scanners captured colour information. As seen in Figure 1, the colour of the surface of the fastener sample plate is consistent, making it possible to use a histogram to sort the points based on their RGB values. Two peaks are identified in the histogram, and the points are divided into two groups. The procedure then follows the same boundary point method and clustering as outlined in previous work.

If colour information is not available, the intensity values use a histogram in a similar way. As previously mentioned, the typical intensity values from such a scanner on a metallic surface often leads to gaps in the point cloud at low incidence angles. The effect of which was minimised by comparing intensities between the plate surface and fasteners on a local level, rather than a one-size-fits-all solution for the full fastener sample plate. However, there were still areas where the intensity values did not differ enough to reliably separate the plate from the fasteners.

Importantly, this algorithm extracted circular features without using a predefined radius. Many prior feature extraction processes depend on a constrained radius is order to eliminate false positives when searching for circular features within a point cloud. Using MSAC-BPD in this work, here with an unconstrained radius, is a novel contribution that allows the algorithm to find holes of multiple radii in the same pass with no prior information.

A further section was added to the algorithm to determine the tilt of each of the fasteners. This was done by extracting the smooth surface of each fastener and treating it like a planar segment. The parameters of the planar segment and the normal direction to the plane were then computed. These values can be used to identify the orientation of each fastener and ensure compliance within the tolerance of the workpiece.

3.2 Scanner A

The fastener sample plate was first scanned using a Scanner A, capturing both sides of the plate. The fastener sample plate was set at the same height as the scanner and was fixed to a precise rotation turn table. A single scan was captured at intervals of 10 degrees, which changed the horizontal incidence angle between the plate normal and the scanner from 0 degrees to 60 degrees. A single scan was captured at each orientation. The range between the scanner and the fastener sample plate was set at one metre.

Both sides of the fastener sample plate were also captured using Scanner B and Scanner C. Given the advertised specifications of each of these instruments, they should both provide a better estimate of the radii of the circles on the surface in question.

3.3 Scanner B

Unlike Scanner A where the incidence angle between the fastener plate and the scanner was changed between setups, with Scanner B the range between the fastener plate and the scanner was changed between single shot scans. The scanner started at a minimum range of 0.3 m from the fastener plate, with a horizontal incidence angle of zero degrees between the scanner and the plate normal. The point cloud was captured from a single setup and then the scanner was moved away from the fastener sample plate at increments of 0.1 m up to a maximum range of 1 m. A single scan was captured at each range. The ranges were measured along a tape measure affixed to the ground of the laboratory. This series of ranges is on the minimum end of Scanner B's range tolerance, which were utilised in order to be able to closely compare the three scanners to each other.

It is important to note that although the horizontal incidence angle between the scanner and the fastener sample plate was controlled as much as physically possible, the vertical incidence angle changed near the edges of the fastener sample plate. Even though the scanner was set at the same height as the sample plate for each single shot scan, the sample plate was large enough and the range between the plate and the scanner was small enough that the incidence angle varied near the edges of the plate. The implications of this effect will be discussed in the results.

Scanner C

Unlike Scanner A and Scanner B, Scanner C is a laser-tracker tracked hand-held triangulation scanner used for reference measurement. The coverage achieved with such a scanner is much more complete than a single setup from a terrestrial scanner, and therefore overcomes the effects of occlusions caused by large incidence angles.

4. Results

This solution focused on optimising incidence angle and range for a single scanning setup of a typical aerospace manufacturing structure. The goal was to determine the most efficient data capture process to produce the best results from a single scan of the fastener sample plate. There are a total of ninety fasteners on the sample plate. On both the aerodynamic and the interior side of the plate, the fasteners have been identified using all three scanners.

Scanner C, a laser-tracker tracked triangulation scanner has been used over a range of hand held angles to the surface to deliver as complete a point cloud as practicable. This allows reference values such as fastener radii to be estimated to an order of magnitude better than scanners A and B. The detection rate for each scanner on both sides of the sample plate will be reported, along with the discrepancy between the estimated radii of Scanner A and Scanner B and the reference radii measured with Scanner C.

4.1 Scanner A

For Scanner A, fasteners have been identified on both the aerodynamic side and the interior side of the fastener sample plate. The detection rate is shown in Table 1. The incidence angle represents the angle between the central rays of the scanner and the normal of the surface of the fastener sample plate. Each of the small, medium and large values is out of a possible thirty detected fasteners, and the detection rate determines the successfully detected fasteners out of a possible ninety.

Incidence angle (˚)	Number of detected fasteners [out of 30]			Detection rate
	Small	Medium	Large	
-60	19	21	21	68%
-50	27	30	25	91%
-40	29	30	25	93%
-30	25	30	23	87%
-20	24	29	24	86%
-10	28	29	29	96%
0	26	29	27	91%
10	28	30	26	93%
20	27	30	30	97%
30	26	30	27	92%
40	27	30	23	89%
50	25	27	26	87%
60	22	22	21	72%

Table 1: Detection rate for aerodynamic side of fastener sample plate, using Scanner A

As expected, there is a drop off in the detection rate as the incidence angle exceeds 50 degrees to the surface normal. There is a high detection rate for all incidence angles up unto that point, with an even distribution across the ninety fasteners on the fastener sample plate.

The quality of the detection can be investigated by determining the difference between the radii of the detected fasteners and their reference values [Figure 3].

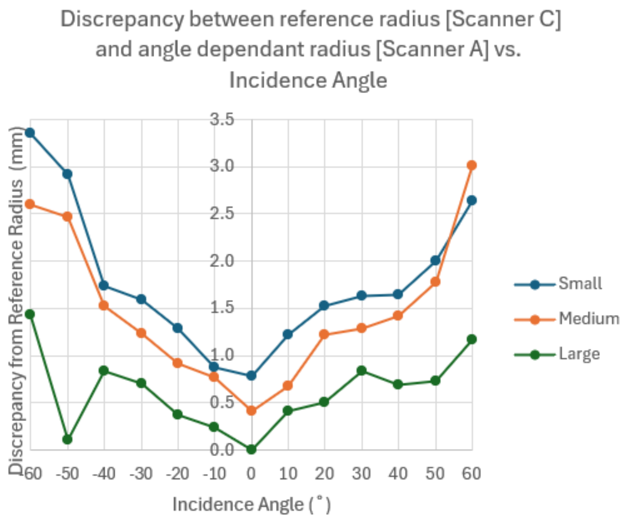

Figure 3: Discrepancy between estimated and reference radii, aerodynamic side, Scanner A

The estimated radius increases with the increasing incidence angle, following a systematic curve. The measurements collected using Scanner A overestimate the radius of the circles when compared to the reference values collected with Scanner C.

The interior side of the fastener sample plate, comprises closely located bolt-shaped fasteners protruding from the planar surface. Fasteners vary in size such that the plate has a systematic set of similar features of increasing dimension. At large incidence angles, the planar surface between each fastener becomes obscured by surrounding fasteners and the individual features can no longer be distinguished from one another. The described geometry is visible in Figure 4, and a sample result is shown in Figure 5.

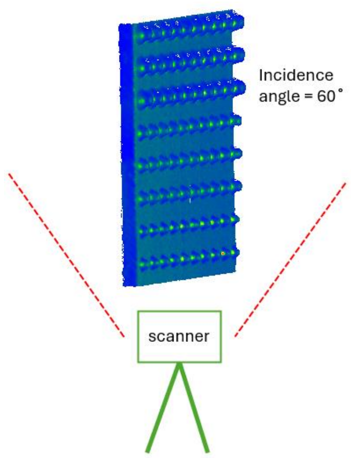

Figure 4: Interior side of the fastener sample plate at incidence angle 60 degrees to the normal

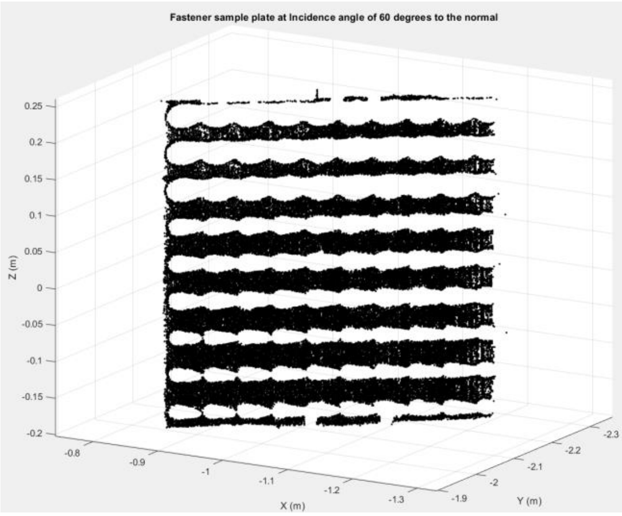

Figure 5: Resulting plane from the interior side of the fastener sample plate at incidence angle 60 degrees to the normal

It is for this reason that the results for the interior side of the fastener sample plate using Scanner A are only shown for the range of -30 degrees to 30 degrees, as any larger incidence angles had significant obscuration to detect individual features. The protrusion of the fasteners from the planar surface caused challenges in individual feature detection, as the bolts created ellipse-like shapes rather than circles. Each fastener obscured the fasteners nearby when the incidence angle was increased. Feature dimensions and proximity between features has a key role in designing scanning setup location for single shot approach - and indeed any approach. The detection rate is presented in Table 2.

Incidence angle (˚)	Number of detected fasteners [out of 30]			Detection rate
	Small	Medium	Large	
-30	12	4	9	28%
-20	24	29	25	87%
-10	26	27	24	86%
0	28	29	30	97%
10	29	30	29	98%
20	28	30	30	98%
30	8	13	15	40%

Table 2: Detection rate for interior side of fastener sample plate, using Scanner A

The best coverage was therefore obtained at low incidence angles due to the full visibility of the fastener sample plate and the dinstinctive separation between fasteners. It is clear that the number of detected fasteners deteriorated quickly as the incidence angle increased. The result shown contributes to identifying an optimal incidence angle for capturing the interior side of such surfaces. Utilising an optimal incidence angle can help to better design the capture and detection processes so that the collection and processing time is minimised, increasing productivity.

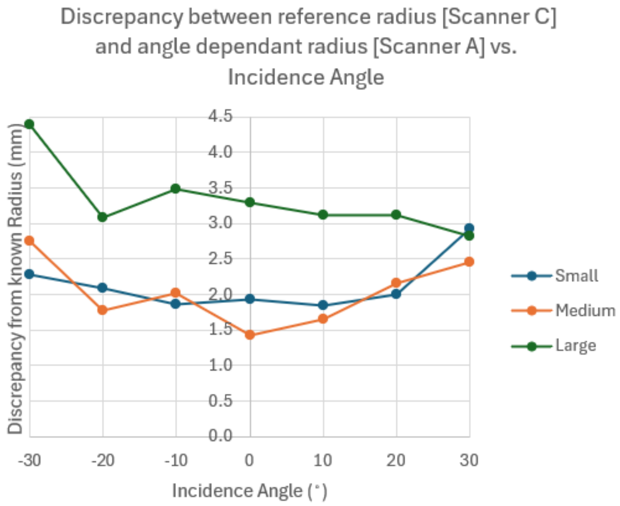

Figure 6: Discrepancy between estimated and reference radii, interior side, Scanner A

Unlike the aerodynamic side of the fastener sample plate, there is no clear trend that the quality of the detected fasteners deteriorates with incidence angle. There is, however, a larger discrepancy between the reference radii of the small, medium and large fasteners and the measured values from Scanner A. This is consistent with the overestimation of the radii seen on the aerodynamic side of the plate.

4.2 Scanner B

The second set of results have a changing range instead of a changing incidence angle. This was to explore the minimum range of a terrestrial laser scanner in order to best compare it to a close-range hand held scanner. The detection rates are presented in Table 3 for the aerodynamic side of the fastener sample plate.

Range (m)	Number of detected fasteners [out of 30]			Detection rate
	Small	Medium	Large	
0.3	8	19	29	62%
0.4	7	16	29	58%
0.5	8	17	30	61%
0.6	6	10	26	47%
0.7	3	8	25	40%
0.8	7	8	26	46%
0.9	5	8	25	42%
1.0	5	12	25	47%

Table 3: Detection rate for aerodynamic side of fastener sample plate, using Scanner B

It is important to note that Scanner B did not collect colour information. This meant that intensity information had to be used in order to identify the fasteners. However, as with any metallic surface, the intensity information will be skewed by the high reflectivity of the surface. In the areas where the scanner was directly perpendicular to the target (incidence angle of zero in all directions), the value of the intensity returns from the surface were so high that it was impossible to distinguish between plate and fastener. This happened on the lower half of the fastener sample plate where the small and medium fasteners were located, seen in Figure 7. In Table 3 it is clear that there is a high amount of the large fasteners detected. This is because they were just off centre of the alignment of the plate and the scanner, giving them an incidence angle slightly larger than zero.

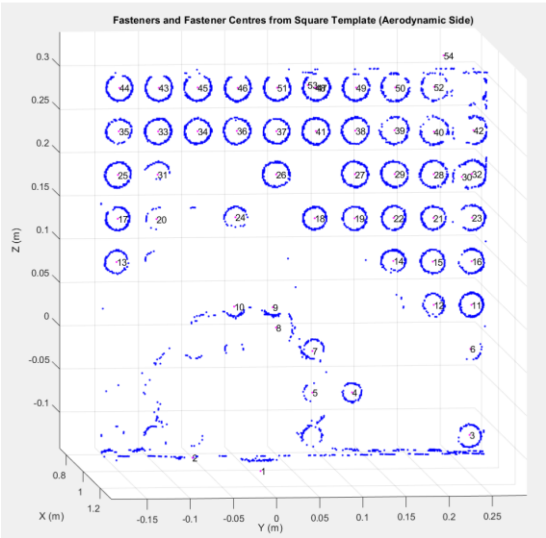

Figure 7: Scanner B on aerodynamic side of fastener sample plate at range 0.3 m

The quality of the results for the aerodynamic side of the fastener sample plate can be found in Figure 8.

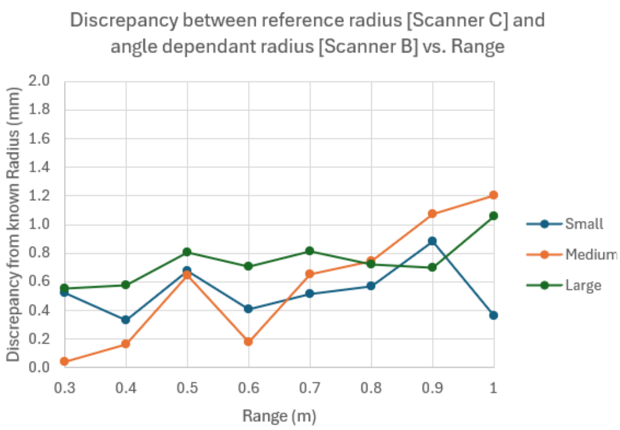

Figure 8: Discrepancy between estimated and reference radii, aerodynamic side, Scanner B

Despite the reduction in detection rate, the fasteners that have been detected are in better accordance with the reference values than those from Scanner A. Again there is slight overestimation in radii, but for the most part the estimated radii of the fasteners are within 1 mm from the reference values. Interestingly, the minimum scanning range of Scanner B is 0.25 m, and the best performance in this test comes from that measurements taken at a range of 0.3 m, near the end of the feasible measuring range.

Lastly, the results from the interior side of the fastener sample plate measured with Scanner B are shown in Table 4.

Range (m)	Number of detected fasteners [out of 30]			Detection Rate
	Small	Medium	Large	
0.3	29	16	1	51%
0.4	28	28	3	66%
0.5	28	24	8	67%
0.6	29	30	20	88%
0.7	30	30	27	97%
0.8	30	30	28	98%
0.9	29	30	28	97%
1.0	30	29	28	97%

Table 4: Detection rate for interior side of fastener sample plate, using Scanner B

Unlike the aerodynamic side of the fastener sample plate, the poorest detection occurs at the minimum range of 0.3 m. As previously described, this is due to the variation in incidence angle and the protruding fasteners obscuring each other, the result of which is visualised in Figure 9.

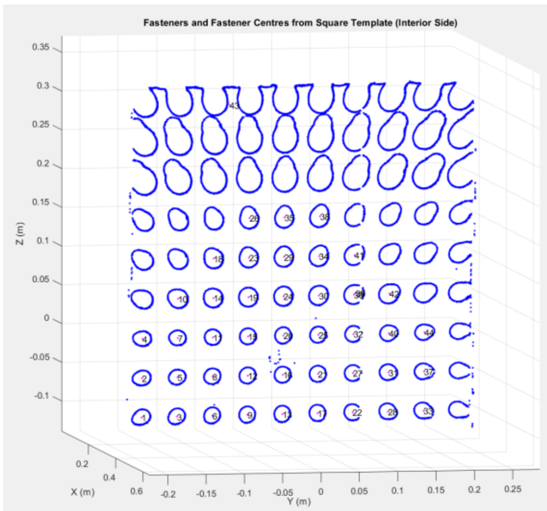

Figure 9: Scanner B on interior side of fastener sample plate at range 0.3 m

The large fasteners at the top of the fastener sample plate form almost elliptical shapes that are highly different from their physical form. As the scanner moves away from the plate and the range increases, the 'vertical' incidence angle gets less severe and the number of detected large fasteners increases. Note that the very strong perspective is due to the scanner proximity to the plate, not an artefact of the projection used in the graphical display. The estimated radii of the detected fasteners is presented in Figure 10.

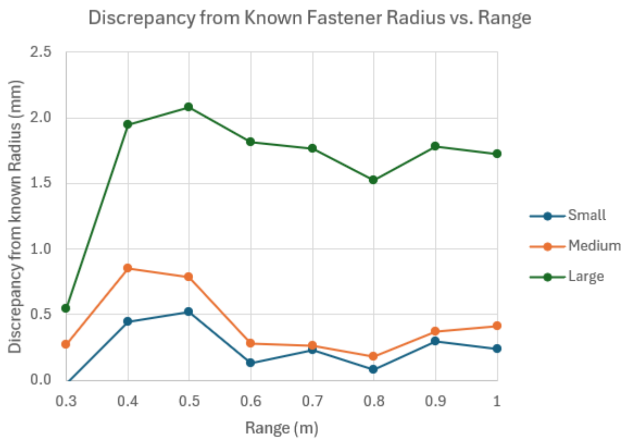

Figure 10: Discrepancy between estimated and reference radii, interior side, Scanner B

The estimated fastener radii for the interior side using Scanner B are the most similar to the reference values from Scanner C. The radii of the small and medium fasteners are within 0.5 mm of the reference value. The consistent overestimation suggests that an additive constant could be utilised in the algorithm to adjust for the boundary point detection method and the edge-based calculation of the radii.

4.3 Precision

Assessing the repeatability of the fastener detection can provide an estimate of the precision of the method. The standard deviations of the estimated fastener radius for Scanner A are presented in Table 5.

Inc. angle (°)	Standard Deviation (mm)					
	Aerodynamic side			Interior side		
	small	med	large	small	med	large
-60	1.59	1.29	1.92			
-50	1.26	1.39	0.95			
-40	0.74	0.50	0.79			
-30	0.61	0.60	0.62	1.61	1.27	1.40
-20	0.58	0.51	0.64	0.94	0.87	1.03
-10	0.57	0.32	0.78	0.68	0.69	0.44
0	0.58	0.66	0.95	0.40	0.37	0.59
10	0.56	0.63	0.95	0.38	0.54	0.25
20	0.71	0.71	0.67	0.63	0.79	0.61
30	0.41	0.70	1.17	2.08	1.62	3.93
40	1.07	0.94	0.70			
50	0.95	0.55	1.50			
60	1.18	1.30	1.43			

Table 5: Standard deviations for both aerodynamic and interior sides of fastener sample plate using Scanner A

For the low incidence angles, the majority of the radii estimates are within 0.5 mm for the small, medium, and large fasteners. Similar to the number of fasteners detected and the quality of the radii estimates, the precision of the estimated radii began to decrease with incidence angles larger than 20 degrees.

The standard deviations of the estimated fastener radius for Scanner B for both the aerodynamic side and the interior side are presented in Table 6.

Range (m)	Standard Deviation (mm)					
	Aerodynamic side			Interior side		
	Small	Med	Large	Small	Med	Large
0.3	0.56	0.71	0.35	0.26	0.27	0.20
0.4	0.69	0.71	0.38	0.25	0.34	0.45
0.5	0.64	0.62	0.44	0.20	0.17	0.27
0.6	0.67	0.85	0.45	0.12	0.18	0.25
0.7	0.37	0.59	0.50	0.11	0.10	0.37
0.8	0.60	0.73	0.47	0.24	0.20	0.29
0.9	0.46	0.52	0.59	0.20	0.40	0.35
1.0	0.87	0.78	0.56	0.19	0.12	0.21

Table 6: Standard deviations for both aerodynamic and interior sides of fastener sample plate using Scanner B

As seen in Table 6, the standard deviations for the radius estimates on the interior side of the fastener sample plate are smaller than those for the aerodynamic side. For Scanner B, the fastener detection on the interior side of the fastener sample plate outperformed Scanner A in both precision and accuracy, and had excellent fastener detection rates above ranges of 0.5 m.

4.4 Further Work

Estimating fastener tilt has been identified as a useful area for future study. Using a similar detection strategy to the detection of the fastener radii, the smooth surface of each fastener on the aerodynamic side of the fastener sample plate can be found. These are often the 'leftover' points from the MSAC-BPD algorithm. These groups of points can be clustered using a simple region growing, and then treated as planar surfaces. For each fastener, the planar parameters and the normal direction can be computed. It is anticipated that the tilt determined by the terrestrial laser scanners will be compared to alternative mechanical and optical solutions.

5. Conclusions

This work is a continuation of previous work on this subject, but with a more complete scenario that is closer to a real factory implementation of the solution. Using a single shot scanning method, a series of tests on range and incidence angle were performed on an aerospace fastener sample plate using two mid-range terrestrial laser scanners. Results were determined by comparing estimated values with a reference data set captured using a laser-tracked hand held laser scanner.

On the whole, Scanner B closely outperformed Scanner A when detecting fasteners from both the aerodynamic and interior side of the fastener sample plate. This result was consistent with published instrument specifications, as Scanner B is designed to have a much smaller working range than that of Scanner A. The quality of the solution was reported holistically by commenting on detection rate, accuracy of radii when compared to a reference, and precision of radii. The systematic overestimation of fastener radii with increasing incidence angle is consistent with previous results obtained in (Pexman and Robson 2022).

Given the presented results, some conclusions can be drawn about optimal range and incidence angle to the normal for the given task. For a single shot setup using a terrestrial laser scanner to capture an aerodynamic surface, the tested range of 0.3-1 m is suitable, and the incidence angle should not exceed 40 degrees from the surface normal. For the same setup on the interior of the aerospace surface, the incidence angle should be constrained to less than 30 degrees, and if possible the range should be larger than 0.5 m.

The authors recognise that these recommendations for range and incidence angle will not always be possible in real manufacturing scenarios. However, the work presented makes valuable contributions to understanding the feasibility of utilising terrestrial laser scanner for high precision metrology tasks in aerospace manufacturing environments. The methods presented in this manuscript displayed eminent capacity for the automated extraction of fasteners from aerospace surfaces, with applications to on-line quality control and monitoring, and dimensional compliance control.

Acknowledgements

This work was conducted with the support of UCL EPSRC scholarship, as well as support from Airbus.

References

Bendels, Gerhard H, Ruwen Schnabel, and Reinhard Klein. 2006. "Detecting Holes in Point Set Surfaces." *Journal of WSCG* 14:8.

Bolkas, D. 2019. "Terrestrial Laser Scanner Intensity Correction for the Incidence Angle Effect on Surfaces with Different Colours and Sheens." *International Journal of Remote Sensing* 40 (18): 7169–89. https://doi.org/10.1080/01431161.2019.1601283.

Bolles, Robert C., and Martin A. Fischler. 1981. "A Ransac-Based Approach to Model Fitting and Its Application to Finding Cylinders in Range Data *." In , 637–43.

Bullen, George. 2013. *Automated/Mechanized Drilling and Countersinking of Airframes*. Pennsylvania, USA: SAE International.

Fischler, Martin A., and Robert C. Bolles. 1981. "Random Sample Consensus: A Paradigm for Model Fitting with Applications to Image Analysis and Automated Cartography." *Communications of the ACM* 24 (6): 381–95. https://doi.org/10.1145/358669.358692.

Kaasalainen, Sanna, Anttoni Jaakkola, Mikko Kaasalainen, Anssi Krooks, and Antero Kukko. 2011. "Analysis of Incidence Angle and Distance Effects on Terrestrial Laser Scanner Intensity: Search for Correction Methods." *Remote Sensing* 3 (10): 2207–21. https://doi.org/10.3390/rs3102207.

Kukko, Antero, Sanna Kaasalainen, and Paula Litkey. 2008. "Effect of Incidence Angle on Laser Scanner Intensity and Surface Data." *Applied Optics* 47 (7): 986. https://doi.org/10.1364/AO.47.000986.

Lozano-Perez, T., W. Grimson, and S. White. 1987. "Finding Cylinders in Range Data." In *Proceedings. 1987 IEEE International Conference on Robotics and Automation*, 4:202–7. Raleigh, NC, USA: Institute of Electrical and Electronics Engineers. https://doi.org/10.1109/ROBOT.1987.1088007.

Lukács, Gabor, Ralph Martin, and Dave Marshall. 1998. "Faithful Least-Squares Fitting of Spheres, Cylinders, Cones and Tori for Reliable Segmentation." In *Computer Vision — ECCV'98*, edited by Hans Burkhardt and Bernd Neumann, 1406:671–86. Lecture Notes in Computer Science. Berlin, Heidelberg: Springer Berlin Heidelberg. https://doi.org/10.1007/BFb0055697.

Mineo, Carmelo, Stephen Gareth Pierce, and Rahul Summan. 2018. "Novel Algorithms for 3D Surface Point Cloud Boundary Detection and Edge Reconstruction." *Journal of Computational Design and Engineering* 6 (1): 81–91. https://doi.org/10.1016/j.jcde.2018.02.001.

Nguyen, Van Sinh, Trong Hai Trinh, and Manh Ha Tran. 2015. "Hole Boundary Detection of a Surface of 3D Point Clouds." In *2015 International Conference on Advanced Computing and Applications (ACOMP)*, 124–29. https://doi.org/10.1109/ACOMP.2015.12.

Pexman, and Robson. 2022. "Registration And Feature Extraction From Terrestrial Laser Scanner Point Clouds For Aerospace Manufacturing." *The International Archives of the Photogrammetry, Remote Sensing and Spatial Information Sciences* XLVIII-2/W2-2022 (December):119–26. https://doi.org/10.5194/isprs-archives-XLVIII-2-W2-2022-119-2022.

Pfeifer, Norbert, Peter Dorninger, Alexander Haring, and Hongchao Fan. 2007. "Investingating Terrestrial Laser Scanning Intensity Data: Quality and Functional Relations," January, 10.

Roth, Gerhard, and Martin Levine. 1993. "Extracting Geometric Primitives." *CVGIP: Image Understanding* 58 (1): 1–22.

Rubio, R., L. Granero, M. Sanz, J. García, and V. Micó. 2017. "Analysis and 3D Inspection System of Drill Holes in Aeronautical Surfaces." In , edited by Peter Lehmann, Wolfgang Osten, and Armando Albertazzi Gonçalves, 1032948. Munich, Germany. https://doi.org/10.1117/12.2270302.

Tang, Hao, Laishui Zhou, Yuanpeng Liu, and Jun Wang. 2022. "Tiny Hole Inspection of Aircraft Engine Nacelle in 3D Point Cloud via Robust Statistical Fitting." *Measurement* 196 (June):111250. https://doi.org/10.1016/j.measurement.2022.111250.

Taubin, G. 1991. "Estimation of Planar Curves, Surfaces, and Nonplanar Space Curves Defined by Implicit Equations with Applications to Edge and Range Image Segmentation." *IEEE Transactions on Pattern Analysis and Machine Intelligence* 13 (11): 1115–38. https://doi.org/10.1109/34.103273.

Wang, Qian, Yi Tan, and Zhongya Mei. 2020. "Computational Methods of Acquisition and Processing of 3D Point Cloud Data for Construction Applications." *Archives of Computational Methods in Engineering* 27 (2): 479–99. https://doi.org/10.1007/s11831-019-09320-4.

Yang, Yi, Hairong Fang, Yuefa Fang, and Shijian Shi. 2020. "Three-Dimensional Point Cloud Data Subtle Feature Extraction Algorithm for Laser Scanning Measurement of Large-Scale Irregular Surface in Reverse Engineering." *Measurement* 151 (February):107220. https://doi.org/10.1016/j.measurement.2019.107220.